Trinity College Dublin
Coláiste na Tríonóide, Baile Átha Cliath
The University of Dublin

School of Computer Science and Statistics

Cardiopulmonary Resuscitation Assistant: Evaluation of the Chest Compression Rate from the Bottom-Up View

Jerico Alcaras
14317110

April 12, 2019

A Dissertation submitted in partial fulfilment
of the requirements for the degree of
MCS (Master in Computer Science)

Declaration

I hereby declare that this project is entirely my own work and that it has not been submitted as an exercise for a degree at this or any other university.

I have read and I understand the plagiarism provisions in the General Regulations of the University Calendar for the current year, found at `http://www.tcd.ie/calendar`.

I have also completed the Online Tutorial on avoiding plagiarism 'Ready Steady Write', located at `http://tcd-ie.libguides.com/plagiarism/ready-steady-write`.

Signed: _____ Date: _____

Abstract

The aim of this research paper is to evaluate the chest compression rate (CCR) from the bottom-up view using a smartphone placed flat on the floor facing upwards. The CCR is to be evaluated in real-time during cardiopulmonary resuscitation (CPR) as a proof-of-concept for the CPR Assistant project.

Out-of-hospital cardiac arrest (OHCA) is a leading cause of mortality globally, with more than 350,000 incidents annually in the United States alone, and a low survival rate of 12%. CPR performed by bystanders has been found to increase rates of survival to one month for victims of OHCA. The rate of bystander CPR can be improved globally, and tools to aid bystander CPR must be made conveniently available. Metrics such as the CCR and the chest compression depth (CCD) are vital metrics for applying quality CPR.

This research paper explores the different aspects of CPR and the recommended procedures. Investigation and analysis is also performed on existing methods of evaluating the CCR, outlining performance and the drawbacks that these solutions incur. This critical analysis justifies the goal of this research paper.

Evaluation of the CCR was performed by developing an algorithm that employs computer vision techniques. This algorithm uses the acceleration of pixels in real-time to detect chest compressions. Artificial ventilation is also detected using the displacement of pixels as a secondary objective.

The algorithm is robust and performs well, detecting 88% of chest compressions and 69% of artificial ventilations in a mixture ideal and non-ideal test environments. This is suitable for use in training scenarios, but must be further refined to realise its full potential. Methods to achieve this are also outlined.

Acknowledgements

I would like to thank my family, and my friends for their continued support in my endeavours. Special thanks to my supervisor Dr. Kenneth Dawson-Howe, Joanna Whittam, Maksim Maiberg and Maksim Lizura for their assistance in this project.

Contents

Abbreviations

AHA	American Heart Association
CCD	Chest compression depth
CCR	Chest compression rate
cpm	compressions per minute
CPR	Cardiopulmonary resuscitation
ms	milliseconds
OHCA	Out-of-hospital cardiac arrest

1 Introduction

1.1 Goal

The primary goal of the cardiopulmonary resuscitation (CPR) assistant project in its entirety is to develop a smartphone application that analyses the administration of CPR in real-time using computer vision techniques while also providing resources for CPR training as a secondary feature. As part of the CPR assistant project, this research paper explores the evaluation of the chest compression rate (CCR) in real-time from the bottom-up view using the front camera of a smartphone placed flat on the floor across the user.

Figure 1.1: The bottom-up view is defined as the perspective of the smartphone (bottom right) when its front camera is used.

1.2 Motivations

The CPR assistant project is motivated by the high global mortality rate of out-of-hospital cardiac arrest and the potential to maximize the rate of bystanders performing CPR. In 2017, the annual report published by the Irish Out-of-Hospital Cardiac Arrest Register recorded 2,333 incidents of out-of-hospital cardiac arrest (OHCA) in Ireland, equivalent to a rate of 49 per 100,000 population [1]. The report also states that 50% of these incidences were bystander-witnessed, with 80% of this subset receiving bystander CPR. The survival rate remains relatively low, with only 6.5% of these patients discharged from the hospital alive. In 2018, the American Health Association (AHA) reported a total of 356,461 cases of OHCA in the United States, equivalent to a rate of 110.8 per 100,000 population [2]. Of these cases, bystander CPR was performed on 45.7% in adults and 61.4% in children. The Pan-Asian Resuscitation Outcomes Study clinical research recorded over 66,000 OHCA cases from multiple Asian countries between 2009 and 2012, with bystander CPR rates ranging from 10.5% to 40.9% and survival-to-hospital-discharge rates ranging from 0.5% to 8.5% [3]. Although the rate of bystander CPR varies by country, in general such rates have ample room for improvement and is relatively low in many countries.

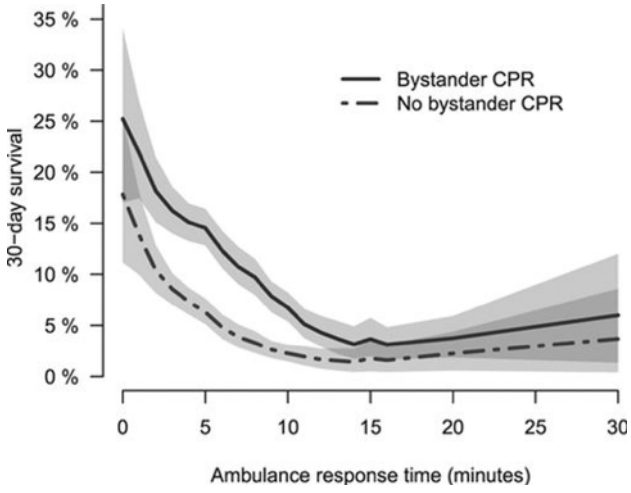

Figure 1.2: One-month survival rate of OHCA patients who were administered bystander CPR versus who were not, factoring in ambulance response time [4].

Bystander CPR has been proven to increase the rate of survival to one month versus no-bystander CPR. In a study conducted in Japan from 2011 to 2012 consisting of 2,157 OHCA patients, a 9.3% survival rate to one month was observed for patients who received compression-only bystander CPR, compared to 3.7% for those who did not [5]. This rate rises to 25.9% for CPR with artificial ventilation, known as conventional CPR. A study in Sweden between 1990 and 2002 revealed that OHCA patients who received bystander CPR from laypeople had a 2.7% greater rate of survival to one month compared to no-bystander CPR [6]. This difference increased to 7% when healthcare professionals administered the

bystander CPR. In a study in Denmark between 2005 and 2011 involving 7,623 OHCA patients, a 22.6% survival rate to one month was observed for those who received bystander CPR within 5 minutes of cardiac arrest, versus 6.7% for those who did not (see Figure 1.2) [4]. This difference tapers with increasing response time. However, the bystander CPR survival rate remained higher than no-bystander for all response time intervals.

Barriers for bystander CPR include fear of doing it incorrectly, fear of liability and fear of endangering one's self [7]. In interviews with 684 bystanders who witnessed OHCA, 37.5% stated panicking as a reason for not performing CPR [8]. Furthermore, 9.1% perceived that they would not be able to do CPR correctly. In a 2017 study conducted in China involving 1,841 laypeople, 74.4% responded as not trained in CPR and 44.4% were worried about inadequate knowledge and skill if faced with the decision of performing CPR [9]. It is clear that the lack of confidence and knowledge is a significant barrier faced by laypeople, and suggests that a solution must be developed to aid in overcoming this barrier.

While survival to one month does not imply survival to hospital discharge, it is an important milestone for long-term survival. It is therefore essential that the rate of bystander participation in CPR be maximised to further improve survival rates for victims of cardiac arrest. Education and training provided by a smartphone application to boost knowledge and confidence coupled with the large rates of smartphone ownership are to be leveraged by the CPR assistant project to achieve this goal, with the ultimate intention of saving lives.

2 Background

2.1 Performing CPR

CPR is an emergency lifesaving procedure performed on those who have suffered cardiac arrest. Cardiac arrest occurs when the heart fails to pump blood, resulting in a sudden loss of blood flow. CPR serves as a procedure to manually pump the heart in order to partially restore the flow of blood to vital organs such as the brain until the return of spontaneous circulation (ROSC) is achieved via defibrillation. The AHA published guidelines for CPR that details the suggested algorithm and technique to be followed in CPR to maximise the chances of survival in cardiac arrest scenarios [10]. Updates to these guidelines were made in 2015, 2017 and 2018.

Figure 2.1: CPR being performed on a patient, accompanied by an automated external defibrillator (AED). Photo courtesy of `www.cprconsultants.com`.

2.1.1 Chest Compressions

The purpose of chest compressions in CPR is to manually pump the heart for partial restoration of blood flow. There are several aspects of chest compressions that must be considered for effective CPR.

For CPR on adults, the heel of one hand is to be placed in the centre of the patient's chest.

The heel of the other hand is then placed on top of it, with the fingers interlaced together. The administrator then pushes down with force on the chest, effectively "compressing" it. For infants, two fingers are placed on the breastbone instead. Straight arms must be maintained during this movement and the patient's chest must be allowed to rise completely before the next compression [11].

2.1.2 Artifical Ventilation

Artificial ventilation (or rescue breaths) are performed to provide oxygen to the patient. The suggested technique is the head-tilt-chin-lift manoeuvre. This is done by placing the palm of one hand on the patient's forehead, gently tilting the head back. The other hand is then used to gently lift the chin forward to open the airway [12].

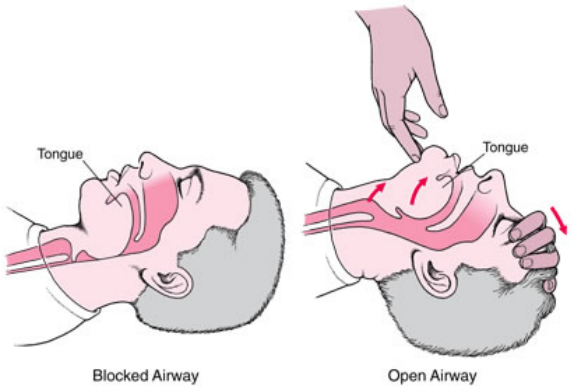

Figure 2.2: Head-tilt-chin-lift manoeuvre. Photo courtesy of `www.cpr-test.org`.

2.1.3 Chest Compression Depth (CCD)

Based on the latest updates made to CPR guidelines in 2018 [13], the AHA recommends that compressions be performed at a depth of at least 2 inches or 5 centimetres for adults, while avoiding a depth exceeding 2.4 inches or 6 centimetres. This depth is referred to as the chest compression depth (CCD). For infants, children and adolescents, the recommended depth is greater than one third of the anteroposterior diameter of the chest. Optimal CCD is important to ensure that enough force is being applied to pump blood to vital organs.

2.1.4 Chest Compression Rate (CCR)

The AHA recommends a rate of 100 to 120cpm (compressions per minute) [13]. This rate is referred to as the chest compression rate (CCR). The CCR is an extremely important aspect of effective CPR. A CCR that is too low provides insufficient blood flow to vital organs. A

CCR that is too high is found to compromise CCD [14], which also may lead to insufficient blood flow.

2.2 Types of CPR

2.2.1 Conventional CPR

Conventional CPR combines chest compressions and artificial ventilation. The AHA suggests that artificial ventilation be performed if the administrator of CPR is trained in conventional CPR [15]. It is also recommended that chest compressions and artificial ventilation be performed at a ratio of 30:2 for adults in cardiac arrest.

2.2.2 Compression-only CPR

Compression-only CPR does not employ the use of artificial ventilation. The AHA recommends performing this type of CPR for those who are untrained or for those who are trained solely in this type of CPR [15].

2.2.3 Two-rescuer CPR

Two-rescuer CPR involves the participation of a second rescuer in CPR. The task of providing chest compressions and artificial ventilation is divided between the two rescuers. The onset of rescuer fatigue in CPR over time significantly affects the correctness of chest compressions, and it is recommended that rescuers swap every two minutes to mitigate the effects of fatigue [16, 17].

Figure 2.3: Two-rescuer CPR. Photo courtesy of `www.emsworld.com`.

2.3 Prior Work

Previous work exists in the domain of CCR evaluation. These employ the use of technologies such as computer vision and smartphone accelerometers.

2.3.1 Using Computer Vision

A 2018 research by Corkery successfully evaluates the CCR from a smartphone video taken from the front view, marking the beginning of the CPR assistant project [18]. This solution employs the use of a computer vision technique known as dense optical flow. Using the displacement of pixels calculated by this algorithm, compressions and artificial ventilations were recognised by the solution. proved to be performant and effective, possessing a total accuracy, precision and recall of 0.99 for chest compression detection. Detection of artificial ventilations had a total accuracy, precision and recall of 0.96, 0.96 and 1, respectively. In addition to this, Corkery implemented an Android application that evaluates the CCR from the front view using the same solution logic as a proof-of-concept. This application also has additional secondary features such as visual feedback, audio feedback and progress tracking. However, the front-view that the algorithm required implies that the smartphone must be propped or held by a third-party to capture the subject. Additionally, the algorithm was not tested in non-ideal scenes and was only tested in ideal scenes containing trivial noise.

Solutions also exist to evaluate the CCR from a bottom-up view using computer vision. A study from 2014 used a video from the bottom-up view taken from a smartphone placed between the manikin and user to evaluate the CCR [19]. The solution implemented by this study used the sum of pixel values for every video frame to create an oscillatory signal for evaluating the CCR. Accuracy of the classification of CCR (correct, too low or too fast) ranged from 80% to 90%. The position of the smartphone however, does not allow the user to view live feedback and information.

A study from 2016 also used a video from the bottom-up view taken from a smartphone to detect the CCR [20], but was placed across the user and manikin instead of between the user and manikin. This position allowed the user to view feedback and information from the phone. The implemented solution used the evaluation of the power spectral density to evaluate the CCR. The algorithm worked well in both ideal and non-ideal situations, but was ineffective if the subject had long loose hair.

2.3.2 Using Accelerometers

Accelerometers are devices used to measure acceleration. Signals from chest acceleration were found to be a very robust and effective method to evaluate the CCR as well as the CCD. A study from 2016 evaluates the CCR using a dedicated accelerometer that was also placed in-between the administrator's hands and the manikin's chest [21]. A displacement sensor was installed in the manikin, and data from this sensor was used as reference for evaluating the accelerometer's output. The acceleration signal was processed using three distinct signal processing techniques: linear filtering, detection of zero-crossing in the velocity signal, and spectral analysis of the acceleration signal. The highest median error rate was 1.7cpm using linear filtering.

A study from 2013 evaluates the CCR through the use of a smartphone's accelerometer [22]. The CCR was evaluated by measuring the time between compressions from the resulting displacement waveform. The root mean square error was 4.53cpm with the phone under the hands, and 4.19cpm using the armband. While this approach is very accurate, it cannot provide live visual feedback and information to the user if the phone is placed under the hands. In addition, it faced issues with accidental presses of hardware buttons. If the armband is used, then it is implied that the purchase and setup of this equipment will be required before use.

2.3.3 Analysis

Although the previous work in this domain provide viable solutions to evaluating the CCR, they face significant logistical impracticalities that impedes the ease of use. The evaluation of the CCR from the bottom-up view using a smartphone placed across the user and adjacent to the patient is the optimal approach, as it enables the user to view live feedback and information. It also does not require purchase and setup of any additional equipment. While a solution already exists using the same position and view, its reliability falters when long loose hair is introduced as a factor. These problems suggest that a more practical and robust solution to evaluate the CCR must be developed, which is what this research paper attempts to provide.

3 Implementation

3.1 Overview

A solution was created by harnessing the acceleration and displacement of pixels and applying thresholds to detect chest compressions and artificial ventilation. Computer vision techniques provided by the OpenCV library [23] were used extensively in implementation. Implementation was completed using Python 3.

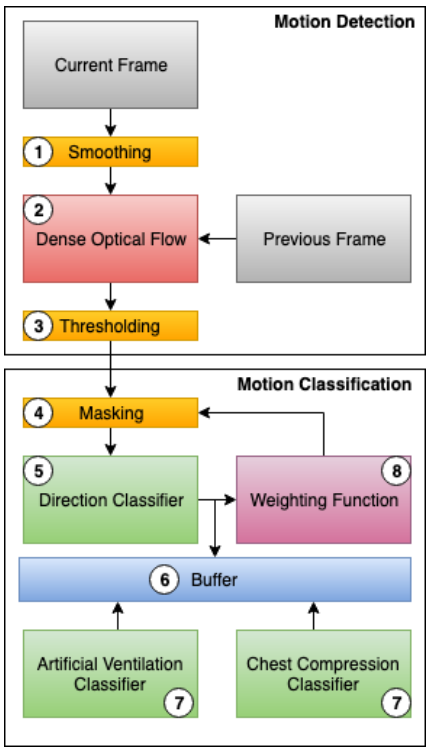

Figure 3.1: A high-level architecture overview of the pipeline.

The solution processes video in real-time. At every frame the following logic is executed (see Figure 3.1 for reference):

1. The current frame is smoothed using a 3x3 blur kernel to reduce image noise.
2. A displacement vector is calculated for every pixel using the previous and current

frame, resulting in a matrix of displacement vectors.

3. A threshold is applied to the displacement matrix to reduce noise.
4. The displacement matrix is masked using normalized weights to isolate the region-of-interest.
5. The displacement matrix are separated into vertical and lateral displacement matrices by the direction classifier.
6. The vertical and lateral displacement matrices are pushed into a buffer.
7. The chest compression and artificial ventilation classifiers independently read the buffer to detect chest compressions and artificial ventilation, respectively.
8. The vertical displacement matrix is passed into the weighting function to calculate new weights for masking the next frame.

3.2 Detecting Motion

The first stage in the pipeline detects movement. Movement in the scene is exploited and forms the basis of detecting chest compressions and artificial ventilation.

3.2.1 Dense Optical Flow

Optical flow is described as the apparent motion vector of objects or surfaces in a scene. It relies on the brightness constancy constraint, which states that a moving pixel in a frame will have the same intensity in the next frame. It also relies on the assumption that adjacent pixels will have similar motion. Given a pixel with intensity I, co-ordinates x and y at time t, it moves with Δx and Δy over time Δt. Following the brightness constancy constraint, its intensity remains the same (Equation 1).

$$\mathrm{I}(x, y, t) = \mathrm{I}(x + \Delta x, y + \Delta y, t + \Delta t) \tag{1}$$

A Taylor-series approximation of the right-hand side, removal of common terms, and division by Δt results in the following equation (Equation 2) [24].

$$f_x u + f_y v + f_t = 0 \;\; \textit{where} \;\; f_x = \frac{\partial f}{\partial x};\; f_y = \frac{\partial f}{\partial y};\; u = \frac{\Delta x}{\Delta t};\; v = \frac{\Delta y}{\Delta t} \tag{2}$$

This resulting equation is known as the optical flow equation. In this equation, f_x and f_y

are known as the image gradients. f_t is known as the gradient over time. However u and v are unknowns, and the presence of two unknown variables indicate that this singular equation is non-trivial to solve.

In computer vision, there are two suggested approaches for solving the optical flow equation. Sparse optical flow (known as the Lucas-Kanade method) calculates the optical flow between two frames using a sparse feature set. This feature set is predetermined using feature detectors. In contrast, dense optical flow calculates the optical flow for all pixels between two frames. OpenCV's implementation of dense optical flow uses Gunnar Farneback's algorithm [25]. For every pixel in every frame, a displacement vector (u, v) is calculated. The resulting vector matrix is used in detecting chest compressions and artificial ventilation.

Figure 3.2: A visualization of dense optical flow during CPR. Hue denotes direction and its brightness denotes magnitude. The change in hue indicates a change in direction. [25]

Dense optical flow was chosen due to the priority of maintaining a high degree of accuracy, and forms the core of the implemented solution. Due to its computationally expensive nature, the optical flow of all pixels in the original frame are not required. Frames were scaled down to a resolution of 256x144 pixels before calculation. This was found to be a good compromise between accuracy and performance.

3.2.2 Noise Reduction

Raw camera video is prone to image noise, which is detected as false movement by the dense optical flow algorithm. To mitigate the effects of image noise on the output of this algorithm, the image is smoothed using an average blur kernel of size 3x3 pixels. After calculating optical flow, thresholding is applied to discard any displacement vectors that have a magnitude of 0.2 pixels or less. A magnitude of such value is considered to be noise

or movement that is not strong enough to be passed on to the next stage in the pipeline. A mask is also applied to the displacement vectors to isolate the region-of-interest, which is the region of the user in the frame.

3.3 Classifying Motion

The second stage in the pipeline detects chest compressions and artifical ventilation by using the displacement vectors calculated from the previous stage to classify motion.

3.3.1 Direction

The motion of chest compressions during CPR can be described as a vertical movement. In comparison, the motion required for artificial ventilation can be described as a lateral movement. In order to classify motion as chest compressions or artificial ventilation, displacement vectors must first be classified by its direction before proceeding with further classification. Using polar angles, a direct upward direction (north) is classified as 90 degrees relative to the positive x-plane. From this, a set of filters were implemented (Table 4.1).

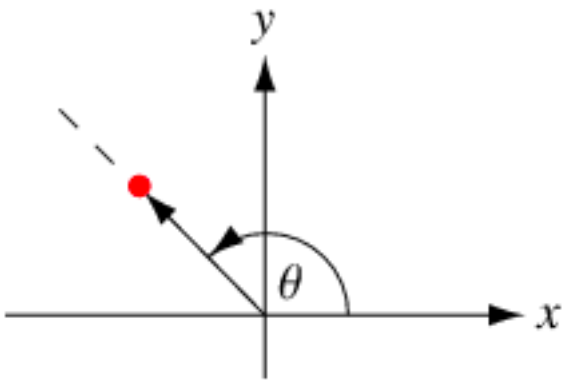

Figure 3.3: Polar angles in the 2D plane [26].

Table 3.1: Filters for classifying displacement vectors by direction.

Condition (deg)	Classification
$30 \leq \theta \ \wedge \ \theta \leq 150$	Up
$210 \leq \theta \ \wedge \ \theta \leq 330$	Down
$160 \leq \theta \ \wedge \ \theta \leq 200$	Left
$340 \leq \theta \ \vee \ \theta \geq 20$	Right

Directions are classified as a range of angles (in degrees), as the movement of the user is not guaranteed to be perpendicular. A boundary of 10 degrees exists between the vertical and horizontal ranges to account for error caused by false classification. Calculation of the horizontal and vertical resultants of each displacement vector was attempted initially to evaluate the true magnitude in each plane, but was considered an unnecessary expense of computation for precision that was not needed. ***For each direction, the displacement vectors are summed to denote the total displacement in that direction for the current frame. The sums for each direction are then pushed to a FIFO buffer with a size equivalent to a user-defined time period in frames. This time period was chosen to be 325ms.***

3.3.2 Chest Compressions & Artificial Ventilation

Once the sum in each direction is pushed to the buffer, the contents in the buffer are utilized to detect chest compressions and artificial ventilation. A chest compression can be described as a strong downward movement followed by a strong upward movement in a very short period of time. Movement for artificial ventilation is a strong lateral movement, followed by a strong lateral movement in the opposite direction (when returning to the position for giving chest compressions). Averages are calculated using the buffer, after which thresholding is applied to detect chest compressions and artificial ventilation.

Using displacement to detect artificial ventilation

Displacement is a vector defined as the overall change in position, and is the output of dense optical flow. It is suitable for detecting artificial ventilation as it is characterised as a strong, infrequent lateral movement. Given the leftward displacement s_{left} and the rightward displacement s_{right}, the total lateral displacement s for a frame is calculated:

$$s = s_{left} + s_{right}$$

This lateral displacement value is computed and pushed to the buffer for every frame. The artificial ventilation classifier then computes an average of the lateral displacement values stored in the buffer. Given a buffer of size t frames and lateral displacement matrix s, the average lateral displacement $\bar{S}_{lat}$ over t frames is calculated as follows:

$$\bar{S}_{lat} = \frac{\sum_{n=0}^{t-1} s_n}{t-1}$$

For the purposes of this research, ***an average lateral displacement of 3000 pixels over***

325ms is classified by the program as artificial ventilation. This state is held continuously until a chest compression is detected.

It was observed that using displacement alone to detect chest compressions was unsuitable when looking from the bottom-up view. The low magnitude of displacement observed from this perspective means that a low threshold value must be used to detect chest compressions. Use of a low threshold value greatly increased the probability of detecting false positives due to noise and unwanted disturbances. Usage of a high threshold value would result in missed compressions. The range of possible threshold values was found to be extremely limited for this case. Thresholds required a flexible range of values so that they may be adjusted depending on the characteristics of the environment e.g. when a scene is noisy the threshold value must be high so as not to detect false positives, but not too high that it will miss compressions.

Using acceleration to detect chest compressions

Chest compressions can be alternatively described as periodic bursts of acceleration. Acceleration is a vector defined as the rate of change in displacement with respect to time. Given the upward displacement s_{up} and the downward displacement s_{down}, the resultant vertical displacement s is calculated:

$$s = s_{up} - s_{down}$$

A negative value denotes a resultant displacement in the downward direction. This resultant value is pushed to the buffer, similar to the artificial ventilation classifier. Using these values, the average vertical displacement $\bar{S}_{vert}$ is then calculated over buffer size t:

$$\bar{S}_{vert} = \frac{\sum_{n=0}^{t-1} s_n}{t-1}$$

This value is also pushed to the buffer. The vertical velocity V_{vert} over t frames is then calculated by computing the change in average displacement between the start and end of the buffer:

$$V_{vert} = \bar{S}_0 - \bar{S}_{t-1}$$

This value is also pushed to the buffer to derive acceleration. The vertical acceleration A_{vert} over t frames is finally calculated by computing the change in velocity between the start and end of the buffer:

$$A_{vert} = V_0 - V_{t-1}$$

A negative acceleration value denotes an acceleration in the downward direction. ***A downward acceleration of 1,500 pixels/s^2 followed immediately by an upward acceleration of 500 pixels/s^2 is classified by the program as a chest compression.*** Once a strong downward acceleration is detected, a window of 750ms is given to detect a strong upward acceleration. This value was chosen for detecting slower rates of CCR. If this window passes and no upward acceleration is detected, it is discarded as noise and the program returns to its original state. The usage of pixel acceleration to detect compressions is suitable as it allowed for a greater range of possible threshold values, due to the significantly higher magnitude observed.

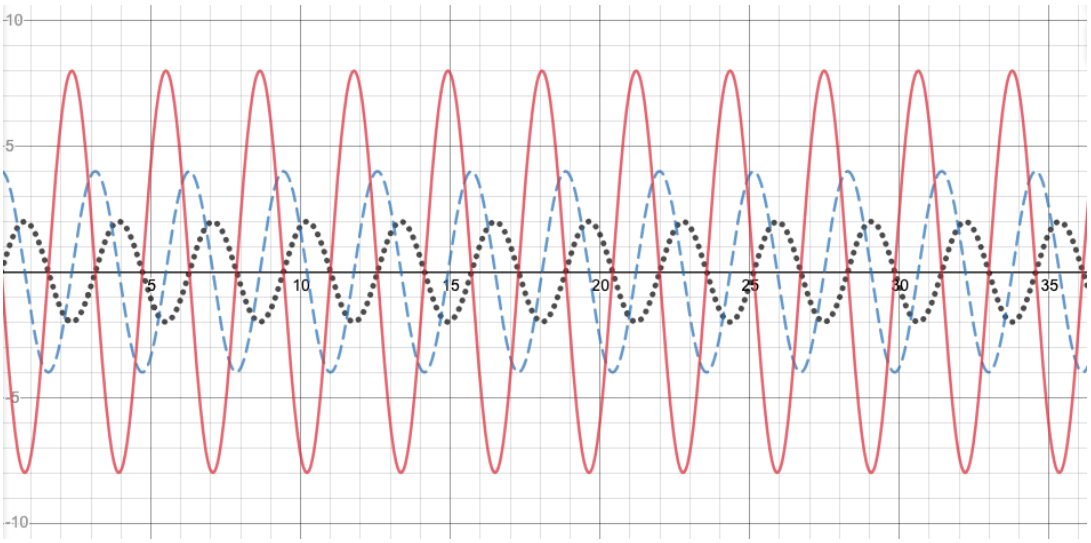

Figure 3.4: Example of a vertical displacement signal (dotted, black line) and its derivatives: velocity (dashed, blue line), and acceleration (solid, red line). Note how acceleration has the greatest amplitude. This can be exploited for a greater range of possible threshold values.

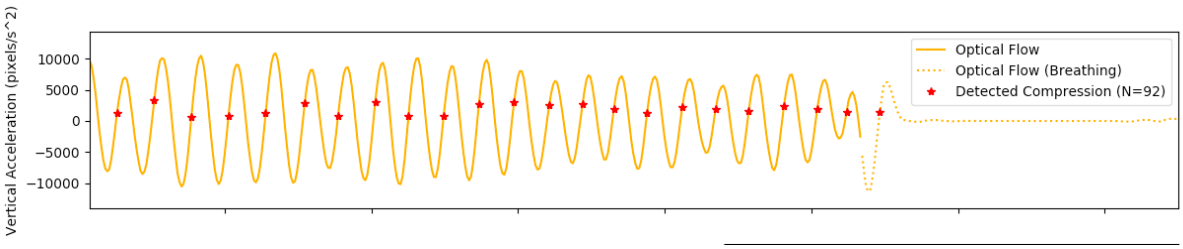

Figure 3.5: Output graph of vertical acceleration over a segment of footage. Negative values denote a downward direction.

3.3.3 Calculating CCR

The CCR is calculated in real-time at every detected compression and uses the time difference between the latest detected and the previous detected compression. Given the time (in seconds from epoch) of the previous detected compression T_{n-1} and the time of the latest detected compression T_n, the formula to calculate the CCR (in compressions per minute) at the nth compression is:

$$CCR_n = \frac{60}{(T_n - T_{n-1})} \quad where \quad n > 1$$

3.4 Weighted Region-of-Interest Model

Figure 3.6: The weighted mask after several seconds of CPR time. Note the increasing weight in the region of the user and diminishment of the non-moving area on the bottom-right.

To mitigate the effects of noise, Corkery's weighted region model [18] was utilised and extended as an effective form of retrieving the region-of-interest. This model gives a greater weighting to regions with a higher density of movement as the CPR procedure progresses. Given the magnitude of vertical displacement u_{vert}, learning rate L, and old weight w_{old}, a new weight w_{new} is calculated as follows:

$$w_{new} = W + (u_{vert} * L) \; where \; W = w_{old} * (1 - L)$$

New weights are calculated for every pixel in every frame using a learning rate experimentally chosen to be 0.0065. New weights are not calculated when the program detects a state of artificial ventilation. The set of newly calculated weights is normalized and used as a mask for the next frame. This ensures that the unwanted effects of any background noise will be mitigated.

Preloaded weights were also implemented as an experimental improvement to Corkery's model. Weights can be saved optionally after a CPR session ends and can be reused optionally at the start of another session. All weights that are preloaded are initialized at half-strength. It also becomes an input in the weighting function as follows:

$$w_{new} = W + (u_{vert} * L) \text{ where } W = w_{old} * (1 - L) + (w_{pre} * L)$$

The preloading of weights is intended to reduce the effects of noise during the earlier stages of the CPR procedure when the weights have not been fully adjusted by the algorithm. In addition, it also serves as an effective heat-zone for detecting movement should the user's position in the frame deviate over time.

4 Evaluation

4.1 Ground Truth

Footage of CPR using a manikin was recorded for evaluation. 13 sessions of CPR totalling approximately 20 minutes of footage were recorded, each aiming for ratio of 30 chest compression to 2 artificial ventilations. For each session, two videos at 30 frames per second were recorded using smartphones (Figure 5.1). Videos of the bottom-up view and the front view were recorded simultaneously at resolutions of 1280x720 pixels and 1920x1080 pixels, respectively. Both videos were synchronized by switching on a light during the start and end of the session. The video was then subsequently trimmed using these two events so that they were of the same length. Data was then extracted from the front view to serve as ground truth. Similarly, data was extracted from the bottom-up view using the implemented solution. This data was compared to ground truth for evaluation.

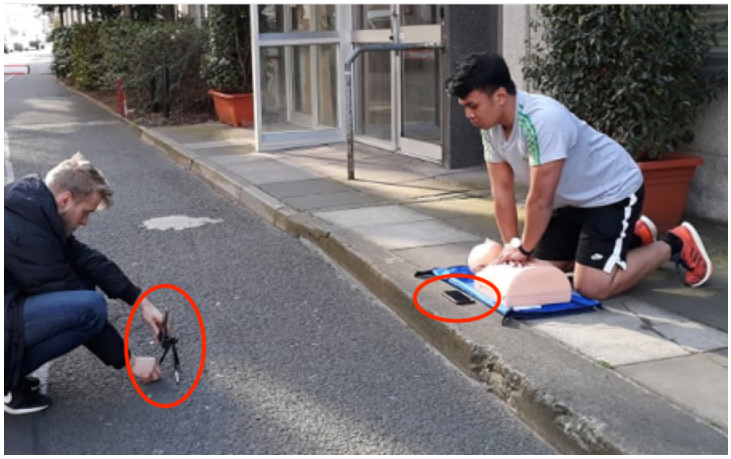

Figure 4.1: Recording CPR footage. A video of the front view was recorded (left) to serve as ground truth. A video of the bottom-up view was recorded for the solution (right).

The required ground truth data that was retrieved from the front view videos are the frame numbers of the lowest point in each chest compression. In each ground truth video, a ball strapped to the subject's wrist was used to extract the required information. The Hough circle detection technique [27] was then used to detect the centre of the ball and its

coordinates (see Figure 5.2). Frames were annotated as a chest compression when the y-coordinates of the centre of the ball reached a local maximum (see Figure 5.3). Frames were annotated as artificial ventilation immediately after the frame in which the subject completes the final chest compression in a set, up to before the next chest compression frame. Annotations for both chest compressions and artificial ventilation were verified by manually iterating through the video on a frame-by-frame basis. By synchronizing and maintaining the same frame rate across both videos, events will occur at almost the exact same frame between the two videos. The latency error created through the syncing of the videos was observed to be 1 or 2 frames, which is trivial.

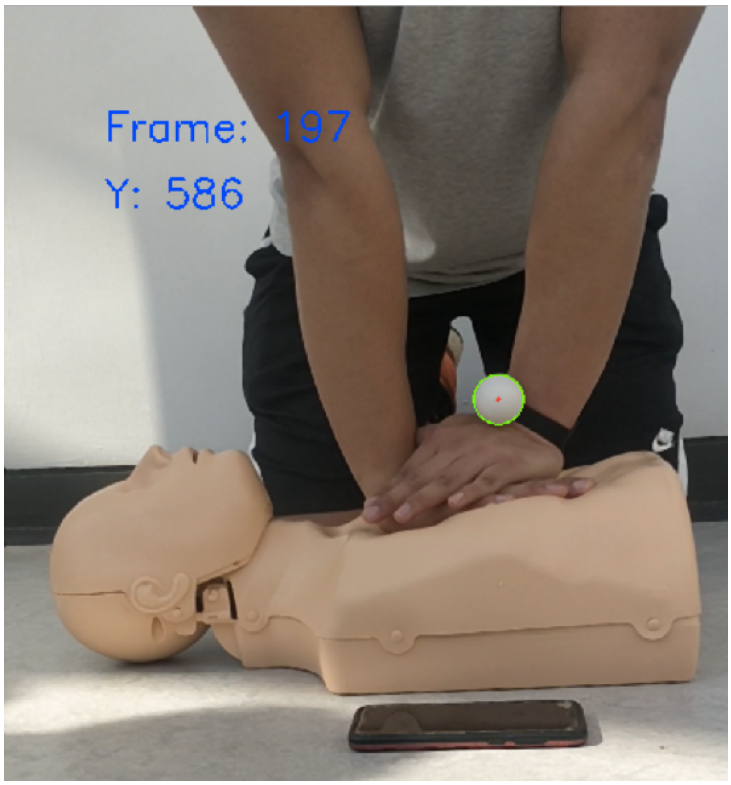

Figure 4.2: Using Hough circle detection to determine ground truth. The green outline denotes the detected circle, and the red dot is its centre. The Y-value on the top left is the Y-coordinate of the red dot in the frame.

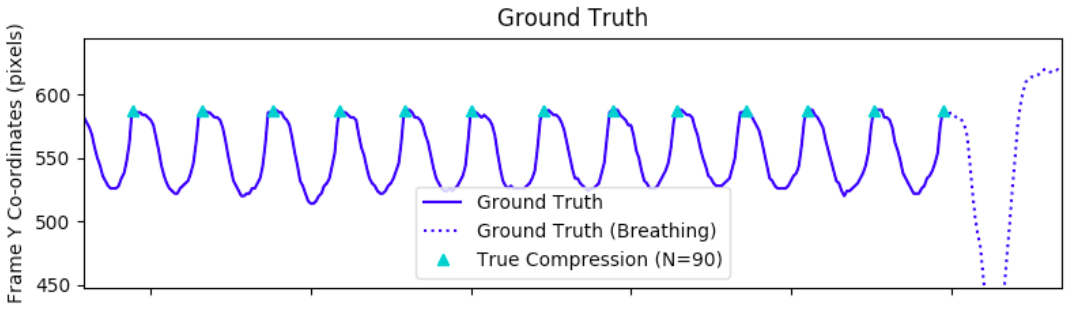

Figure 4.3: A graph visualizing ground truth data over a segment of footage. Chest compressions occur at the peaks due to a flipped coordinate system while using OpenCV.

4.2 Evaluation Metrics

4.2.1 Accuracy, Precision & Recall

The metrics used to evaluate the performance of the solution are accuracy, precision and recall. These metrics were found to be suitable for evaluation due to the solution's binary data classification model [28]. For example, the chest compression classifier determines if acceleration data is a chest compression or not, which is binary. This logic also applies to the artifical ventilation classifier. Evaluation classes were retrieved from the confusion matrix, a table used for evaluating classification performance. The number of instances per evaluation class were counted and substituted into the relevant formulae.

Table 4.1: Evaluation classes used [28]. True negatives are not applicable for this solution.

Class		Meaning
TP	**True Positive**	An actual chest compression that occurred and was detected by the solution.
TN	**True Negative**	A chest compression that did not actually occur and was not detected by the solution (not applicable).
FP	**False Positive**	A chest compression that did not occur but was detected by the solution.
FN	**False Negative**	An actual chest compression that occurred but was not detected by the solution.

$$Accuracy = \frac{TP}{TP + FP + FN}$$

$$Precision = \frac{TP}{TP + FP}$$

$$Recall = \frac{TP}{TP + FN}$$

4.2.2 Mean CCR

The mean CCR was calculated for both the ground truth and the solution. These were compared to evaluate similarity. The formula to calculate the CCR at the nth chest compression given the time (in seconds from epoch) of the previous detected compression T_{n-1} and the time of the latest detected compression T_n:

$$CCR_n = \frac{60}{(T_n - T_{n-1})} \quad where \quad n > 1$$

Note that the CCR requires two points in time, so the CCR at the first encountered chest compression cannot be evaluated. Using the aforementioned equation, the mean CCR (denoted by μCCR) over k chest compressions is calculated by summing the CCR values calculated at every chest compression, then dividing the sum by k minus the first chest compression:

$$\mu CCR = \frac{\sum_{n=2}^{k} CCR_n}{k - 1}$$

4.3 Test Cases

Footage was recorded with different real-world cases to test the solution's robustness. These cases were also combined with each other in some videos to add rigour.

Table 4.2: Letter codes to denote a condition in the CPR footage.

Code	Test Case
L	Subject has long, loose hair.
S	Subject has short hair.
B	Background disturbances wholly intended to disrupt performance.
C	Crop at neck-level (the subject's neck-level and below is cropped out).

Figure 4.4: Different test cases and their letter codes. Disturbances consist of individuals waving, vaping and/or moving in the background (top right).

4.4 Results

Visualizations for results are available online at
`http://cpr-assistant.herokuapp.com/`.

4.4.1 Chest Compressions

Table 4.3: Accuracy, precision and recall for chest compressions.

Dataset	TP	FP	FN	Accuracy	Precision	Recall
L.1	89	6	1	0.93	0.94	0.99
L.2	86	15	3	0.83	0.85	0.97
L.3	83	9	1	0.89	0.90	0.99
S.1	89	7	1	0.92	0.93	0.99
S.2	88	4	2	0.94	0.96	0.98
S.3	89	8	1	0.91	0.92	0.99
S.4	88	5	2	0.93	0.95	0.98
LB.1	89	11	1	0.88	0.89	0.99
LB.2	88	13	1	0.87	0.87	0.99
LB.3	85	10	5	0.85	0.89	0.94
SB	84	8	6	0.87	0.92	0.94
SC	76	5	14	0.80	0.92	0.84
SCB	86	4	4	0.92	0.96	0.96
Overall	**1120**	**105**	**42**	**0.88**	**0.91**	**0.96**

Table 4.4: Mean CCR values (in cpm) for ground truth and solution.

Dataset	$\mu\text{CCR}_{\text{GT}}$	$\mu\text{CCR}_{\text{SLTN}}$	Difference
L.1	102.77	99.92	2.85
L.2	112.2	108.17	4.03
L.3	83.49	81.53	1.96
S.1	71.52	71.95	0.43
S.2	109.09	107.42	1.67
S.3	103.49	99.98	3.51
S.4	112.1	108.25	3.85
LB.1	104.36	98.28	6.08
LB.2	120.43	114.24	6.19
LB.3	117.57	112.86	4.71
SB	110.59	104.48	6.11
SC	103.67	95.85	7.82
SCB	99.81	96.05	3.76
μ			**4.07**

The results for chest compressions are good, but there is room for improvement. Given the low magnitude of movement observed from the bottom-up view, the solution detects chest compressions at a relatively high degree of accuracy even in non-ideal environments. The average of the differences in mean CCR for every video was 4.07cpm, which is fairly good given that the window of ideal CCR is 100cpm to 120cpm. False negatives were attributed to movement not meeting the threshold, due to disturbances or weak movement. False positives mostly occurred in videos testing the case of long, loose hair because of the hair accelerating in the same pattern of movement as chest compressions. Some false positives were attributed to movements before and after sets of compressions when the subject is moving into position for the next compression or when switching on the light at the start and end of the video for syncing.

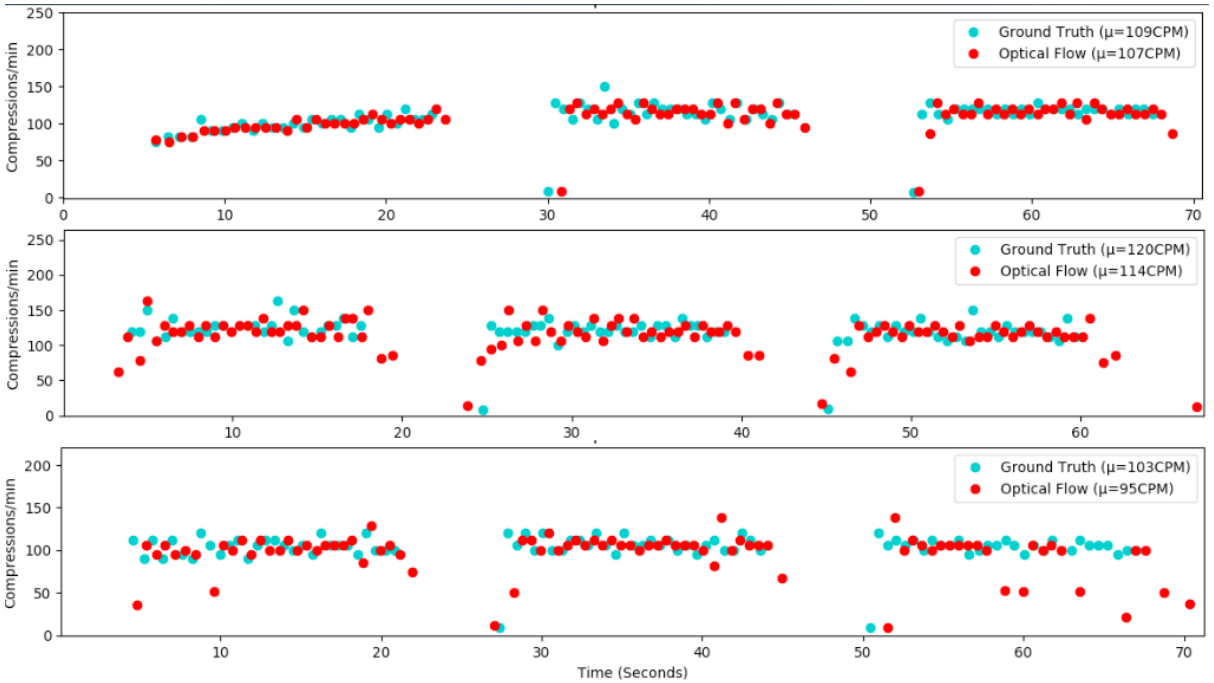

Figure 4.5: Scatter plots of true vs detected chest compressions over time, with CCR. From top to bottom: S.2, LB.2 and SC.

4.4.2 Artificial Ventilation

The results for artificial ventilation are fairly good. No artificial ventilations were missed, which resulted in a perfect recall of 1. False positives were attributed to the lateral movement of long, loose hair being recognised by the solution as a lateral movement for artificial ventilation. The main point to note is that evaluation of artificial ventilation is a secondary objective of this research paper. The artificial ventilation classifier operates independently of the chest compression classifier and does not affect the CCR if an incorrect detection occurs.

Table 4.5: Accuracy, precision and recall for artificial ventilation.

Dataset	TP	FP	FN	Accuracy	Precision	Recall
L.1	2	0	0	1	1	1
L.2	3	3	0	0.5	0.5	1
L.3	3	3	0	0.5	0.5	1
S.1	2	0	0	1	1	1
S.2	2	0	0	1	1	1
S.3	2	0	0	1	1	1
S.4	2	0	0	1	1	1
LB.1	3	1	0	0.75	0.75	1
LB.2	3	4	0	0.43	0.43	1
LB.3	3	3	0	0.5	0.5	1
SB	2	0	0	1	1	1
SC	2	0	0	1	1	1
SCB	2	0	0	1	1	1
Overall	**31**	**14**	**0**	**0.69**	**0.69**	**1**

5 Conclusion

5.1 Critical Analysis

5.1.1 Strengths

- **Robust and performs well in non-ideal environments**. The solution was tested in non-ideal environments and maintained a relatively high degree of accuracy. This is a good start towards a solution that will operate in real-life OHCA scenarios where not all environments will be ideal.
- **Works well with low-resolution images.** This could be vital for performance on low-powered devices such as smartphones, where the frames will have to be scaled down from the native resolution to achieve acceptable frame rates.
- **Allows two-rescuer CPR to be performed.** The position of the smartphone combined with the robustness of the solution means that two-rescuer CPR may be performed freely and with predictably similar accuracy, though the logic of artificial ventilation classification may require slight modifications.

5.1.2 Weaknesses

- **The position may crop out essential parts of the user.** Accuracy suffers if insufficient movement is provided by the user, most especially if parts of the user are cropped out due to, for example, the presence of the patient's arms. The user may have to exaggerate movement if the shoulder-level and below is cropped out due to such obstructions or incorrect placement. This could potentially affect the user's technique in performing chest compressions.

5.2 Viability

Based on results, it is indeed viable to evaluate the CCR from the bottom-up view at a relatively high degree of accuracy. However, parameters for detecting chest compressions and artificial ventilation need to be tuned for optimal performance. The thresholds used for classification were manually chosen through trial-and-error and observation of outputs using the videos. In spite of this, the slight inaccuracies outweigh the benefits of the smartphone's position during use. It allows CPR to be performed easily without any setup and also allows for visual feedback to be displayed to the user. An important point to note is that it is intended for use in training scenario, therefore a certain degree of error can be accepted. While its viability is proven, the solution requires more testing and tuning to harness its full potential.

6 Future Work

6.1 Adaptive Thresholding

Parameters such as the threshold values that are used by the chest compression and artificial ventilation classifiers are constant. These thresholds should be adjusted on a per-scene basis, since not all environments are the same. These parameters should be changed dynamically depending on the characteristics of the scene e.g. depending on the noise observed in the scene, the program may choose to increase the threshold value to a more optimal value that will mitigate the risk of false positives.

6.2 Mobile Application

The solution should be ported to mobile platforms such as Android and iOS in the form of a mobile application with features similar to Corkery's proof-of-concept [18]. This will require rigorous testing and adjustment so that it is optimized for different chipsets. Not all smartphones have the same hardware, and due to the fact that this is a computer vision problem, slight modifications may be needed to ensure the same performance across all devices.

6.3 CCD Evaluation

The evaluation of the CCD from the same view could be investigated. This would require the use of a front-facing camera that has depth detection. The combination of CCR and CCD detection from the bottom-up view's position coupled with audiovisual feedback could be a revolution in CPR training.

Bibliography

[1] *OHCAR Annual Report 2017*, 2017. [Online]. Available: `https://www.nuigalway.ie/media/collegeofmedicinenursinghealthsciences/disciplines/generalpractice/files/OHCAR-Annual-Report-2017.pdf`, [Accessed 6 April 2019].

[2] E. Benjamin *et al.*, "Heart disease and stroke statistics—2018 update: A report from the american heart association," *Circulation*, vol. 137, p. 74, Apr. 2019.

[3] M. Ong *et al.*, "Outcomes for out-of-hospital cardiac arrests across 7 countries in Asia: The Pan Asian Resuscitation Outcomes Study (PAROS)," *Resuscitation*, vol. 96, pp. 100–108, 2015.

[4] S. Rajan *et al.*, "Association of bystander cardiopulmonary resuscitation and survival according to ambulance response times after out-of-hospital cardiac arrest," *Circulation*, vol. 134, no. 25, pp. 2095–2104, 2016.

[5] T. Fukuda *et al.*, "Conventional versus compression-only versus no-bystander cardiopulmonary resuscitation for pediatric out-of-hospital cardiac arrest," *Circulation*, vol. 134, no. 25, pp. 2060–2070, 2016.

[6] J. Herlitz, L. Svensson, S. Holmberg, K. Ängquist, and M. Young, "Efficacy of bystander CPR: Intervention by lay people and by health care professionals," *Resuscitation*, vol. 66, no. 3, pp. 291–295, 2005.

[7] C. Sasson, J. Haukoos, C. Bond, M. Rabe, S. Colbert, R. King, M. Sayre, and M. Heisler, "Barriers and facilitators to learning and performing cardiopulmonary resuscitation in neighborhoods with low bystander cardiopulmonary resuscitation prevalence and high rates of cardiac arrest in Columbus, OH," *Circulation: Cardiovascular Quality and Outcomes*, vol. 6, no. 5, pp. 550–558, 2013.

[8] R. Swor, I. Khan, R. Domeier, L. Honeycutt, K. Chu, and S. Compton, "CPR training and CPR performance: Do CPR-trained bystanders perform CPR?," *Academic Emergency Medicine*, vol. 13, no. 6, pp. 596–601, 2006.

[9] M. Chen, Y. Wang, X. Li, L. Hou, Y. Wang, J. Liu, and F. Han, *Public Knowledge and Attitudes towards Bystander Cardiopulmonary Resuscitation in China*. BioMed Research International, 2017.

[10] *CPR & ECC Guidelines – ECC Guidelines*. [Online]. Available: `https://eccguidelines.heart.org/index.php/circulation/cpr-ecc-guidelines-2/`, [Accessed 6 April 2019].

[11] *What Is Hands-Only CPR?* [Online]. Available: `https://www.webmd.com/first-aid/cardiopulmonary-resuscitation-cpr-treatment#1-3`, [Accessed 6 April 2019].

[12] *Cardiopulmonary resuscitation (CPR): First aid*. [Online]. Available: `https://www.mayoclinic.org/first-aid/first-aid-cpr/basics/art-20056600`, [Accessed 6 April 2019].

[13] A. Panchal *et al.*, "2018 American Heart Association focused update on advanced cardiovascular life support use of antiarrhythmic drugs during and immediately after cardiac arrest: An update to the american heart association guidelines for cardiopulmonary resuscitation and emergency cardiovascular care," *Circulation*, vol. 138, no. 23, 2018.

[14] J. K. Russell *et al.*, *Abstract 17983: Optimal Chest Compression Rate During CPR: The Importance of Filling Time*. [Online]. Available: `https://www.ahajournals.org/doi/10.1161/circ.134.suppl_1.17983`, [Accessed 6 April 2019].

[15] M. Kleinman *et al.*, "2017 American Heart Association focused update on adult basic life support and cardiopulmonary resuscitation quality: An update to the american heart association guidelines for cardiopulmonary resuscitation and emergency cardiovascular care," *Circulation*, vol. 137, no. 1, 2018.

[16] C. McDonald, J. Heggie, C. Jones, C. Thorne, and J. Hulme, "Rescuer fatigue under the 2010 ERC guidelines, and its effect on cardiopulmonary resuscitation (CPR) performance," *Emergency Medicine Journal*, vol. 30, no. 8, pp. 623–627, 2012.

[17] F. Ochoa, E. Ramalle-Gómara, V. Lisa, and I. Saralegui, "The effect of rescuer fatigue on the quality of chest compressions," *Resuscitation*, vol. 37, no. 3, pp. 149–152, 1998.

[18] G. Corkery and K. Dawson-Howe, *"A Smartphone Tool for Evaluating Cardiopulmonary Resuscitation (CPR) Delivery"*. Cardiopulmonary Resuscitation Assistant, 2018.

[19] A. Frisch *et al.*, "Analysis of smartphone video footage classifies chest compression rate during simulated CPR," *The American Journal of Emergency Medicine*, vol. 32, no. 9, pp. 1136–1138, 2014.

[20] K. Engan, T. Hinna, T. Ryen, T. Birkenes, and H. Myklebust, "Chest compression rate measurement from smartphone video," *BioMedical Engineering OnLine*, vol. 15, no. 1, 2016.

[21] S. R. D. Gauna, D. M. González-Otero, J. Ruiz, and J. K. Russell, "Feedback on the rate and depth of chest compressions during cardiopulmonary resuscitation using only accelerometers," *Plos One*, vol. 11, no. 3, 2016.

[22] T. Amemiya and T. Maeda, "Poster: Depth and rate estimation for chest compression cpr with smartphone," *2013 IEEE Symposium on 3D User Interfaces (3DUI)*, p. 125–126, 2013.

[23] *OpenCV Library*. [Online]. Available: `https://opencv.org/`, [Accessed 6 April 2019].

[24] *Optical Flow*. [Online]. Available: `https://docs.opencv.org/3.4/d7/d8b/tutorial_py_lucas_kanade.html`, [Accessed 6 April 2019].

[25] G. Farnebäck, "Two-frame motion estimation based on polynomial expansion," *Image Analysis Lecture Notes in Computer Science*, p. 363–370, 2003.

[26] *Polar Angles*. [Online]. Available: `http://mathworld.wolfram.com/PolarAngle.html`, [Accessed 6 April 2019].

[27] *Hough Circle Transform*. [Online]. Available: `https://docs.opencv.org/3.4/d4/d70/tutorial_hough_circle.html`, [Accessed 7 April 2019].

[28] H. M and S. M.n, "A review on evaluation metrics for data classification evaluations," *International Journal of Data Mining & Knowledge Management Process*, vol. 5, no. 2, p. 01–11, 2015.